Designing microbial consortia with defined social interactions

Designing Microbial Consortia with Defined Social Interactions

Wentao Kong[1,2], David R. Meldgin[2,3], James J. Collins[5,6,7,*], and Ting Lu[1,2,3,4,*]

Department of Bioengineering[1], Carl R. Woese Institute for Genomic Biology[2], Department of Physics[3], Center for Biophysics and Quantitative Biology[4], University of Illinois at Urbana-Champaign, Urbana, IL 61801, USA. Institute for Medical Engineering and Science, Department of Biological Engineering, and Synthetic Biology Center[5], Massachusetts Institute of Technology; Broad Institute of MIT and Harvard[6], Cambridge, MA 02142, USA; Wyss Institute for Biologically Inspired Engineering[7], Harvard University, Boston, MA 02115, USA

Correspondence and requests for materials should be addressed to T.L. (luting@illinois.edu) J.J.C. (jimjc@mit.edu).

Abstract

Designer microbial consortia are an emerging frontier in synthetic biology that enables versatile microbiome engineering. However, the utilization of such consortia is hindered by our limited capacity in rapidly creating ecosystems with desired dynamics. Here we present the development of synthetic communities through social interaction engineering that combines modular pathway reconfiguration with model creation. Specifically, we created six two-strain consortia with each possessing a unique mode of interaction, including commensalism, amensalism, neutralism, cooperation, competition and predation. These consortia follow distinct population dynamics with characteristics determined by the underlying interaction modes. We showed that models derived from two-strain consortia can be used to design three- and four-strain ecosystems with predictable behaviors, and further extended to provide insights into community dynamics in space. This work sheds light on the organization of interacting microbial species, and provides a systematic framework—social interaction programming—to guide the development of synthetic ecosystems for diverse purposes.

Introduction

Designer microbial consortia are communities of rationally designed, interacting microorganisms that are capable of producing desired behaviors[1-4]. In the past decade, an array of such synthetic systems were developed, enabling different applications such as generating specific ecological dynamics[5-9], promoting species growth[10,11] and synthesizing valuable chemicals[12,13]. Compared to engineered isogenic populations, synthetic communities offer an increased degree of robustness for designed cellular functions and an expanded spectrum of functional programmability for complex tasks, thereby enabling novel and versatile biotechnological applications in complex settings[1]. Synthetic microbial consortia have also emerged as a promising engineering tool to manipulate microbiomes, such as those in the human body and in the rhizosphere, which helps to realize the enormous potential of microbiomes for therapeutic, environmental, and agricultural purposes[14-17]. However, despite increasing exciting proof-of-concept demonstrations, the utilization of such synthetic ecosystems is hampered by our limited ability in rapidly developing microbial ecosystems with desired temporal and spatial dynamics.

Cellular social interactions, such as competition and cooperation, are ubiquitous in microbial communities and shown to be essential in specifying ecosystem dynamics[18]. For instance, engineering cross feeding offers species co-existence[10,19,20] while building predator-prey interactions can lead to oscillatory, bistable or mono-stable behaviors[6]. Inspired by these findings, here we present a systematic framework to the design, construction and characterization of synthetic microbial communities, namely, social

interaction programming that combines modular pathway reconfiguration with model creation. Specifically, we employed a modular pathway reconfiguration approach to create six distinct consortia whose dynamics is specified by their underlying interaction modes. Using a modular approach similar to our experimental construction, we also derived quantitative models that captured experimentally observed population patterns. We further showed that the models from two-strain consortia can be used to design and build three- and four-strain ecosystems with predictable behaviors, and extended our investigations to yield insights into spatial community dynamics. Together, we established social interaction engineering as an effective and valuable route for ecosystem programming.

Results

Modular pathway reconfiguration for programing social interactions

Synthetic gene circuits are typically constructed from the bottom up by assembling individual DNA parts[21-26]; in principle, they can also be created through modular reconfiguration of existing gene clusters (Fig. 1a). Although having been barely practiced, modular cluster reconfiguration can be powerful for rapid circuit engineering due to the increasing complexity of desired functionalities[27] and the high modularity of native gene networks[28]. Inspired by this concept, we harnessed the modular biosynthesis pathways of nisin and lactococcin A (lcnA) in *Lactococcus lactis* (Fig. 1b) to develop programmable cells that could form the basis for synthetic microbial consortia. Of note, nisin, an antimicrobial and quorum-sensing molecule, is encoded by an eleven-gene cluster involving five functional modules, including precursor production,

translocation and initial modification, secondary modification, immunity and signaling[29] (Fig. 1c); and IcnA is an antimicrobial peptide whose underlying pathway consists of precursor production, translocation and immunity modules[30] (Fig. 1d).

The functional modularity of the pathways allowed us to rapidly generate different social interactions by selecting and tuning the molecules' signaling and bactericidal features through the alteration of module combinations. Specifically, we were able to create six synthetic microbial consortia that collectively enumerate all possible modes of pairwise social interactions[18,31-33] (Fig. 1e).

Engineering consortia with unidirectional interactions

We started by constructing a two-strain consortium of commensalism within which one benefits the other. Using our previously developed synthetic biology platform[34,35], we generated one strain (CmA) by introducing into *L. lactis* (NZ9000) the full nisin pathway and the constitutively expressed tetracycline resistance gene (tet^R). We also created the other (CmB) by transforming into NZ9000 a reconfigured version of the nisin pathway, which contains only the signaling and immunity modules, and a nisin-inducible tet^R expression circuit (Fig. 2a and Supplementary Fig. 1). Here, CmA was designed to secrete nisin to trigger the expression of tet^R in CmB, thereby conferring tetracycline resistance on CmB. Additionally, we inserted constitutively expressed fluorescent protein genes, *gfpuv* and *mCherry*, into the strains for observation and analysis.

As anticipated, CmA grew by itself in the GM17 media containing tetracycline due to its constitutive tet^R expression; in contrast, CmB by itself did not grow, as its resistance is not autonomous (Fig. 2b). However, CmA and CmB both grew when co-cultured (1:1 ratio) (Fig. 2b), suggesting that the presence of CmA conferred a growth benefit to CmB. Such behaviors were also observed in a variant of the consortium where the tet^R expression of CmA is nisin-inducible (Supplementary Fig. 2a). Additional experiments showed that CmB grew in the tetracycline-containing media when nisin is supplemented (Supplementary Fig. 2b) but failed to grow when CmA's nisin production is abolished (Supplementary Fig. 2c). Furthermore, we showed that CmB growth was not due to tetracycline degradation or absorption by CmA (Supplementary Fig. 3). Together, these results confirmed that the mechanism of commensalism is the tetracycline resistance of CmB induced by nisin released from CmA. Notably, as CmA and CmB were constructed from the same parental strain (NZ9000), they had an indirect nutrient competition during co-culture, and CmA had a reduced saturation density compared to the case of monoculture.

We next engineered a consortium of amensalism, where one strain adversely affects the other, by leveraging the bactericidal nature of nisin. Specifically, we created one strain (AmA) by transplanting into NZ9000 the full nisin pathway and the other strain (AmB) by simply introducing the vector pCCAMβ1 (Fig. 2d and Supplementary Fig. 1). Again, fluorescence protein genes (*gfpuv* and *mCherry*) were introduced as reporters. We found that, individually, AmA and AmB both grew up to saturation in GM17 media; however, when co-cultured, only AmA was able to grow (Fig. 2e), demonstrating the

existence of a deleterious effect from AmA on AmB. Mechanistically, this effect arose from AmA's production of nisin that inhibits the growth of AmB. Utilizing the bactericidal nature of lcnA, we also constructed another version of amensalism by loading the lcnA pathway to NZ9000 to create a new toxin producer (AmA2) (Supplementary Figs. 4a and 1). Subsequent culturing experiments (Supplementary Fig. 4b) confirmed that the new ecosystem indeed involves one-way deleterious interaction.

We further constructed a two-strain consortium of neutralism, as a control to commensalism and amensalism, by loading to NZ9000 the vector (pCCAMβ1) and reporters (*gfpuv* and *mCherry*) (Fig. 2g and Supplementary Fig. 1). The two resulting strains, NeA and NeB, were able to grow both individually and together (Fig. 2h), confirming that their social interaction is indeed neutral. Notably, the reduction of each strain's saturation density in co-culture was due to indirect nutrient competition.

To quantitatively describe the observed behaviors, we constructed a mathematical framework for two-strain community dynamics using ordinary differential equations (Online Methods and Supplementary Note 1). The framework involves five variables, including two for the strain populations, two for the interacting molecules produced by the strains, and one for the nutrient in culture (Supplementary Eq. S1). In concert with the modular configurability of the bacteriocin pathways for gene circuit development, this modeling framework allows modular alterations to describe specific types of ecosystems. Upon data fitting, four derived models (Supplementary Note 4) successfully captured the population-dynamics characteristics of the consortia of

commensalism (Fig. 2c), amensalism (Fig. 2f and Supplementary Fig. 4c) and neutralism (Fig. 2i).

Developing consortia with bidirectional interactions

Leveraging the modularity of the nisin and lcnA pathways, we next created consortia involving two-way social interactions, namely cooperation, competition and predation. Cooperation is the process where multiple species work together to accomplish a task that yields mutual benefit. To create such a consortium, we designed the common task as nisin production, a multi-step process including precursor production, translocation and post-translational modification (Fig. 1c). The task was divided by assigning one strain (CoA) to synthesize and secrete nisin precursor and the other (CoB) to convert the precursor in the extracellular milieu into active nisin. Tetracycline resistance was chosen as the benefit for completing the task. We developed these two strains by modularly reconfiguring the nisin pathway and introducing nisin-inducible tet^R and reporter systems (Fig. 3a and Supplementary Fig. 1).

Our growth experiments showed that CoA and CoB did not grow in tetracycline-supplemented GM17 media unless they were co-cultured (Fig. 3b). For comparison, each of the strains was able to grow when the media was supplemented with nisin (Supplementary Fig. 5a). Additionally, abolishing the function of either strain (e.g., precursor translocation by CoA and modification by CoB) resulted in no growth of either strain (Supplementary Fig. 5b, c). These results demonstrated the necessity of cooperation for the growth of the engineered strains.

Competition is an interaction between species in which the fitness of one is lowered by the presence of another. We designed an ecosystem with such an interaction by utilizing the antimicrobial features of nisin and lcnA. Experimentally, we generated two competing strains, named CpA and CpB, by introducing the nisin and lcnA pathways into NZ9000 separately (Fig. 3d and Supplementary Fig. 1). Notably, CpA and CpB are essentially the same as AmA and AmA2 (the two versions of toxin producers for amensalism), because competition is the superposition of two counter-oriented, detrimental interactions. We found that CpA and CpB both followed a logistic growth pattern individually but, when co-cultured, CpA grew with a significant time delay (12 hrs) and CpB failed to grow (Fig. 3e) indicating that the fitness of the both strains was reduced with their mutual presence. In this case, CpA won the competition and dominated the population. Notably, although CpB lost the contest, lcnA it released at the beginning of the experiment caused the growth delay and reduction of CpA in co-culture.

It has been theoretically predicted that differential outcomes may arise in competition by altering ecosystem parameters such as relative interaction strengths[36]. To test these predictions, we generated multiple variants of CpA and CpB by tuning their bacteriocin productivities, including CpA2 (a lowered translation initiation rate (TIR) of nisB), CpB2 (a wild-type TIR of lcnA) and CpB3 (an increased TIR of lcnA) (Supplementary Tables 1 and 2). Using different combinations of the variants, we indeed observed distinct competition outcomes including CpB dominance (Supplementary Fig. 6a) and close contests (Supplementary Fig. 6b, c).

Predation is a social interaction where one species (prey) benefits another (predator) while being harmed. It is topologically equivalent to the combination of two unidirectional interactions, commensalism and amensalism, with opposite orientations. In light of this equivalence, we established a community of predation by assigning CmA of commensalism, a nisin producer with constitutive tetracycline resistance, as prey (PrA) and combining the circuits of CmB (nisin-inducible tet^R) and AmA2 (constitutive lcnA production) to form a predator (PrB) (Fig. 3g and Supplementary Fig. 1). In this design, PrA provides the benefit of tetracycline resistance to PrB by secreting nisin, while PrB hurts PrA through the release of lcnA.

When the resulting strains were co-cultured, PrA grew in the first 8 hours but gradually declined to a steady density afterwards, while PrB grew poorly at the beginning but faster later and eventually dominated the population, opposite to the monoculture where PrA grew normally but PrB failed to grow (Fig. 3h). The results confirmed the presence of the predatory relation between PrA and PrB, with the former serving as the prey and the latter as the predator. A variant of the ecosystem with similar behaviors involves the replacement of constitutive tetracycline resistance in PrA with nisin inducibility (Supplementary Fig. 7a). In addition, we confirmed that, in this relationship, both the beneficial and deleterious interactions are mandatory, through the monoculture experiments with nisin supplementation (Supplementary Fig. 7b) and the co-culture experiments where PrA or PrB was replaced by a neutral strain (Supplementary Fig. 7c, d)

To achieve a quantitative understanding of the above two-way ecosystems, we reconfigured our mathematical framework to create three ecosystem models (Supplementary Note 1). Consistent with the experiments, these models were able to generate distinct community dynamics for the cases of cooperation (Fig. 3c), competition (Fig. 3f and Supplementary Fig. 6d-f) and predation (Fig. 3i). Together, the mathematical modeling and experimental development of synthetic ecosystems demonstrated that social interaction engineering is a versatile and effective way to create desired two-strain microbial consortia.

Model-guided design of three- and four-strain ecosystems

To further illustrate the utility of our engineering method, we applied it to tackle a key challenge in microbiome and synthetic ecosystem research, namely, to design complex ecosystems with predictable dynamics. Specifically, we combined our established experimental consortia with mathematical models to determine if the dynamics of complex communities (e.g., three- and four-strain ecosystems) could be predicted from the behaviors of simple two-strain ecosystems. Using the models extended modularly from the two-strain cases (Supplementary Note 2), we first predicted the dynamic behaviors of eight three-strain microbial ecosystems formed by introducing third strains into the existing two-strain consortia. Importantly, in the process of model extension and dynamics prediction, all of the parameters from the two-strain communities remained fixed. The only new parameters were the growth rates of the newly introduced strains (i.e., the third strains), which had not been previously characterized.

To test the model predictions, we experimentally constructed eight third strains (CoAg, CoBg, CpAg, CpBg, CmAg, CmBg, AmAg, and AmBg) in alignment with our models (Online Methods; Supplementary Table 1; Supplementary Note 2). These third strains were derived from the corresponding parent strains in the two-strain consortia (CoA, CoB, CpA, CpB, CmA, CmB, AmA, and AmB) by using a colorimetric reporter gene (*gusA*) to substitute the fluorescence reporter genes (*gfpuv* or *mCherry*). Therefore, the third strains have identical interaction modes as their ancestors, but different growth rates due to the alteration of their reporter systems. For instance, CoAg has the same cooperation features as CoA but a different growth.

After measuring the growth rates of the third strains, we mixed them with the two-strain consortia to form the eight three-strain communities, and performed ecosystem culture experiments (Online Methods). Figure 4 shows the comparison of the model predictions (lines) and experimental measurements (circles) of the eight three-strain ecosystems, which demonstrates that the models successfully predicted the dynamics of the synthetic communities. Notably, the dynamics of these communities can be explained by analyzing their social interaction networks. For instance, in the AmA-AmB-CpAg consortium (Fig. 4c), AmA and CpAg both grew but AmB went extinct because AmA and CpAg both produced nisin that suppressed AmB; in contrast, in the AmA-AmB-CpBg consortium (Fig. 4d), all strains went extinct due to the fact that AmA produced nisin inhibiting both CpBg and AmB and CpBg produced lcnA that suppressed AmA and AmB.

We further tested the feasibility of predicting complex community behaviors from the knowledge of two-strain consortia in selected four-strain ecosystems. Similar to the three-strain cases, we extended the modeling framework to describe four four-strain communities formed through combinatorial strain mixing (Supplementary Note 2). Again, the only new parameters in the models were the growth rates of the newly introduced strains. In parallel, we experimentally developed three new strains, PrBn, CmBn and AmBn, by removing the fluorescence reporter genes of the strains PrB, CmB and AmB, respectively (Online Methods and Supplementary Table 1). Using the new and previous strains, we generated four four-strain ecosystems, performed their co-culture experiments, and further compared the measured population dynamics with the model predictions (Fig. 5). These findings show that the models derived from the two-strain ecosystems successfully predicted the dynamics of more complex, four-strain ecosystems.

Although complex communities may involve higher-order interactions, the agreement between the model predictions and experimental measurements in Figs. 4 and 5 demonstrated that, at least for the ecosystems primarily containing pairwise interactions such as those tested, their community dynamics can be derived from the behaviors of simpler consortia. Additionally, these results affirmed that social interaction engineering is an effective approach to program complex synthetic communities with desired dynamics.

Spatial dynamics of three symmetrical ecosystems

In natural habitats, microbial communities such as the human gut microbiome and the rhizosphere microbiome often extend across space where cellular interactions are subject to the diffusion of interacting molecules[37]. This motivated us to examine whether social interactions play a similar role in spatial settings by using the consortia with symmetrical interactions—neutralism, cooperation and competition—as examples. Using a computational model involving reaction-diffusion equations (Online Methods and Supplementary Note 3), we simulated the development of spatial structures of the three ecosystems whose initial cells were randomly seeded. Our results (Supplementary Figs. 8a and 9a) showed that strains (NeA and NeB) formed random patterns in neutralism with their detailed cell distributions subject to initial seeding, relative abundance and growth rates; for the case of cooperation, the strains (CoA and CoB) tended to be co-localized in space and the patterns developed better with close initial ratios than biased; in competition, homogeneous patterns of a single strain (CpA or CpB) emerged. Spatially averaged statistics of the initial and final populations in the three cases (Supplementary Fig. 8b) further suggested that the ecosystem population ratio drifts unidirectionally in neutralism, converges in cooperation, and diverges in competition.

To test these model predictions, we performed a series of spatial patterning experiments using droplets of well-mixed consortia with varied strain ratios (90:1 to 1:90) but a fixed total density (OD_{600}=0.2) (Online Methods). Consistent with the modeling predictions, the strains within individual colonies were randomly distributed

when neutral, co-localized in cooperation, and mutually excluded in competition (Fig. 6a and Supplementary Fig. 9b). For comparison, we also examined the spatiotemporal dynamics of the predation consortium, which showed an initial ratio-dependent pattern that is distinct from the symmetrical cases (Supplementary Fig. 10).

For the case of cooperation, spatial patterns were better developed with close initial ratios than with unbalanced ratios. However, we also noticed that CpB (red) in the competing consortium dominated in the spatial structures at the 1:1 ratio, contradicting the culture experiment where CpA (green) won the contest (Fig. 3e). We speculated that the discrepancy arose from the different diffusibilities of nisin and lcnA caused by the stronger hydrophobicity of the former, which was confirmed by the patterning experiments on agar plates supplemented with Tween 20, a surfactant promoting nisin diffusion (Supplementary Fig. 11a). For the same reason, the initial ratio separatrices of the other three competing ecosystems all shifted towards a higher nisin producer abundance (Supplementary Fig. 11b, c).

We further compared the relative abundances of the three symmetric consortia during pattern developments. Similar to the modeling analysis, the experimental results (Fig. 6b) showed that the NeA fraction of the neutral consortium increased over time for all initial conditions, the CoA fraction of the cooperative consortium converged towards 91% (i.e., 10:1 ratio), and the CpA fraction of the competitive consortium diverged (either 100% or 0%) with the transition occurring between 3:1 and 1:1. For comparison, population ratio changes in additional cases of competition were also calculated

(Supplementary Fig. 11d-g). To quantify our findings, we further computed the entropy, a measure of the diversity of an ecosystem, and the intensity correlation quotient (ICQ), a measure of strain co-localization in space, of the experimentally observed (Fig. 6c) and simulated patterns (Supplementary Fig. 11h, i). These results pointed to the existence of opposite population driving forces exerted by cooperation that promotes coexistence and by competition favoring mutual exclusion.

In addition to well-mixed colonies, we investigated community organization in structured environments where droplets of individual strains are spaced with varying distances (Supplementary Fig. 12a-c and Online Methods). For neutralism, we found that the strains (NeA and NeB) always coexisted. For cooperation, the strains (CoA and CoB) coexisted but their patterns decayed with the spacing from the well-mixed filled circles (0 mm), to back-to-back domes (3 mm) and to diminishing edges (5 mm). For competition, emerged patterns shifted from one-strain exclusive circles (0mm) to repelled two-strain domes (3 mm) and to full circles (5 mm) with the increase of droplet distance. For comparison, additional cases of competition were also experimentally tested (Supplementary Fig. 12d-g). The results confirmed that social interactions continue to serve as a driving force in structured settings; meanwhile, spatial factors, such as colony spacing in this case, function as additional regulators that modulate pattern emergence.

Discussion

With increasing appreciation of microbiomes' profound impacts on human health, environment and agriculture, understanding and manipulating complex microbial ecosystems has become a defining mission for microbiome science. Our study provides fundamental insights into the structure, dynamics and ecology of interacting microbial species by characterizing synthetic consortia that serve as well-defined abstractions of native communities. In addition, our work demonstrates that social interaction engineering, through the combination of modular pathway reconfiguration and model creation, is a systematic strategy to design ecosystem behaviors. Such a synthetic biology approach sets the stage for creating complex, community functions for a variety of applications. For example, toward microbial cell factories, social interaction programming can be utilized to build the population stability of multiple synthetic strains co-involved in the division of labor in chemical synthesis by introducing cross feeding or differentiating substrate utilizations; such augmented stability will boost the robustness and yield of chemical production during microbial fermentation. Social interaction engineering also enables to establish synthetic ecosystems with predictable temporal and spatial dynamics, which can serve as a controllable tool to systematically perturb microbiomes and further alter their structure and dynamics in a desired manner. Looking forward, as microbes inhabit primarily complex, natural environments, our engineering strategy will become more versatile by validating the translatability of its applications from well-controlled, laboratory conditions to realistic settings.

Methods

Methods, including statements of data availability and any associated accession codes and references, are available in the online version of the paper.

Acknowledgements

We thank M. Sivaguru, G. Fried and A. Cyphersmith for their help with colony imaging at the IGB Core Facilities at UIUC, and B. Pilas of the Roy J. Carver Biotechnology Center at UIUC for assistance with flow cytometry analysis in this study. We also thank H. Liu, W. van der Donk, X. Yang and A. Blanchard for stimulating discussions and help. This work was supported by the National Science Foundation (1553649, 1227034), the Office of Naval Research (N000141612525), the American Heart Association (12SDG12090025), the Center for Advanced Study at UIUC, National Center for Supercomputing Applications, the Paul G. Allen Frontiers Group, and the Defense Threat Reduction Agency (HDTRA1-14-1-0006).

Author Contributions

T.L. and J.J.C. designed the study; T.L. conceived the project; W.K. performed the experiments and collected the data; D.R.M. and T.L. developed the computational models; W.K., D.R.M. and T.L. analyzed the data; T.L., J.J.C., W.K. and D.R.M. discussed the results and wrote the paper.

Competing financial interests

The authors declare no competing financial interests.

References

1. Brenner, K., You, L. & Arnold, F.H. Engineering microbial consortia: a new frontier in synthetic biology. *Trends Biotechnol.* **26**, 483-489 (2008).
2. Großkopf, T. & Soyer, O.S. Synthetic microbial communities. *Curr. Opin. Microbiol.* **18**, 72-77 (2014).
3. De Roy, K., Marzorati, M., Van den Abbeele, P., Van de Wiele, T. & Boon, N. Synthetic microbial ecosystems: an exciting tool to understand and apply microbial communities. *Environ. microbiol.* **16**, 1472-1481 (2014).
4. Bittihn, P., Din, M.O., Tsimring, L.S. & Hasty, J. Rational engineering of synthetic microbial systems: from single cells to consortia. *Curr. Opin. Microbiol.* **45**, 92-99 (2018).
5. Weber, W., Daoud-El Baba, M. & Fussenegger, M. Synthetic ecosystems based on airborne inter-and intrakingdom communication. *Proc. Natl. Acad. Sci. USA* **104**, 10435-10440 (2007).
6. Balagaddé, F.K. et al. A synthetic *Escherichia coli* predator–prey ecosystem. *Mol. Syst. Biol.* **4**, 187 (2008).
7. Chen, Y., Kim, J.K., Hirning, A.J., Josić, K. & Bennett, M.R. Emergent genetic oscillations in a synthetic microbial consortium. *Science* **349**, 986-989 (2015).
8. Gore, J., Youk, H. & Van Oudenaarden, A. Snowdrift game dynamics and facultative cheating in yeast. *Nature* **459**, 253 (2009).
9. Chuang, J.S., Rivoire, O. & Leibler, S. Simpson's paradox in a synthetic microbial system. *Science* **323**, 272-275 (2009).

10. Mee, M.T., Collins, J.J., Church, G.M. & Wang, H.H. Syntrophic exchange in synthetic microbial communities. *Proc. Natl. Acad. Sci. USA* **111**, E2149-E2156 (2014).

11. Wintermute, E.H. & Silver, P.A. Emergent cooperation in microbial metabolism. *Mol. Syst. Biol.* **6**, 407 (2010).

12. Zhou, K., Qiao, K., Edgar, S. & Stephanopoulos, G. Distributing a metabolic pathway among a microbial consortium enhances production of natural products. *Nat. Biotechnol.* **33**, 377-383 (2015).

13. Minty, J.J. et al. Design and characterization of synthetic fungal-bacterial consortia for direct production of isobutanol from cellulosic biomass. *Proc. Natl. Acad. Sci. USA* **110**, 14592-14597 (2013).

14. Hood, L. Tackling the microbiome. *Science* **336**, 1209-1209 (2012).

15. Cho, I. & Blaser, M.J. The human microbiome: at the interface of health and disease. *Nat. Rev. Genet.* **13**, 260-270 (2012).

16. Falkowski, P.G., Fenchel, T. & Delong, E.F. The microbial engines that drive Earth's biogeochemical cycles. *Science* **320**, 1034-1039 (2008).

17. Berendsen, R.L., Pieterse, C.M. & Bakker, P.A. The rhizosphere microbiome and plant health. *Trends Plant Sci.* **17**, 478-486 (2012).

18. Faust, K. & Raes, J. Microbial interactions: from networks to models. *Nat. Rev. Microbiol.* **10**, 538-550 (2012).

19. Shou, W., Ram, S. & Vilar, J.M. Synthetic cooperation in engineered yeast populations. *Proc. Natl. Acad. Sci. USA* **104**, 1877-1882 (2007).

20. Brenner, K., Karig, D.K., Weiss, R. & Arnold, F.H. Engineered bidirectional communication mediates a consensus in a microbial biofilm consortium. *Proc. Natl. Acad. Sci. USA* **104**, 17300-17304 (2007).

21. Hasty, J., McMillen, D. & Collins, J.J. Engineered gene circuits. *Nature* **420**, 224-230 (2002).

22. Endy, D. Foundations for engineering biology. *Nature* **438**, 449-453 (2005).

23. Andrianantoandro, E., Basu, S., Karig, D.K. & Weiss, R. Synthetic biology: new engineering rules for an emerging discipline. *Mol. Syst. Biol.* **2**, 2006.2008 (2006).

24. Arkin, A. Setting the standard in synthetic biology. *Nat. Biotechnol.* **26**, 771-773 (2008).

25. Brophy, J.A. & Voigt, C.A. Principles of genetic circuit design. *Nat. Methods* **11**, 508-520 (2014).

26. Collins, J.J. et al. Synthetic biology: How best to build a cell. *Nature* **509**, 155-157 (2014).

27. Purnick, P.E. & Weiss, R. The second wave of synthetic biology: from modules to systems. *Nat. Rev. Mol. Cell Biol.* **10**, 410-422 (2009).

28. Hartwell, L.H., Hopfield, J.J., Leibler, S. & Murray, A.W. From molecular to modular cell biology. *Nature* **402**, C47-C52 (1999).

29. Lubelski, J., Rink, R., Khusainov, R., Moll, G. & Kuipers, O. Biosynthesis, immunity, regulation, mode of action and engineering of the model lantibiotic nisin. *Cell. Mol. Life Sci.* **65**, 455-476 (2008).

30. Stoddard, G.W., Petzel, J.P., Van Belkum, M., Kok, J. & McKay, L.L. Molecular analyses of the lactococcin A gene cluster from *Lactococcus lactis* subsp. *lactis* biovar diacetylactis WM4. *Appl. Environ. Microbiol.* **58**, 1952-1961 (1992).

31. West, S.A., Diggle, S.P., Buckling, A., Gardner, A. & Griffin, A.S. The social lives of microbes. *Annu. Rev. Ecol. Evol. Syst.* **38**, 53-77 (2007).

32. Foster, K.R. Social behaviour in microorganisms. in *Social Behaviour: Genes, Ecology and Evolution* 331-356 (Cambridge Univ. Press, Cambridge, 2010).

33. Xavier, J.B. Social interaction in synthetic and natural microbial communities. *Mol. Syst. Biol.* **7**, 483 (2011).

34. Kong, W., Kapuganti, V.S. & Lu, T. A gene network engineering platform for lactic acid bacteria. *Nucleic Acids Res.* **44**, e37 (2016).

35. Kong, W. & Lu, T. Cloning and optimization of a nisin biosynthesis pathway for bacteriocin harvest. *ACS Synth. Biol.* **3**, 439-445 (2014).

36. Volterra, V. Variations and fluctuations of the number of individuals in animal species living together. *ICES J. Mar. Sci.* **3**, 3-51 (1928).

37. Nadell, C.D., Drescher, K. & Foster, K.R. Spatial structure, cooperation and competition in biofilms. *Nat. Rev. Microbiol.* **14**, 589-600 (2016).

Figures and Captions

Figure 1

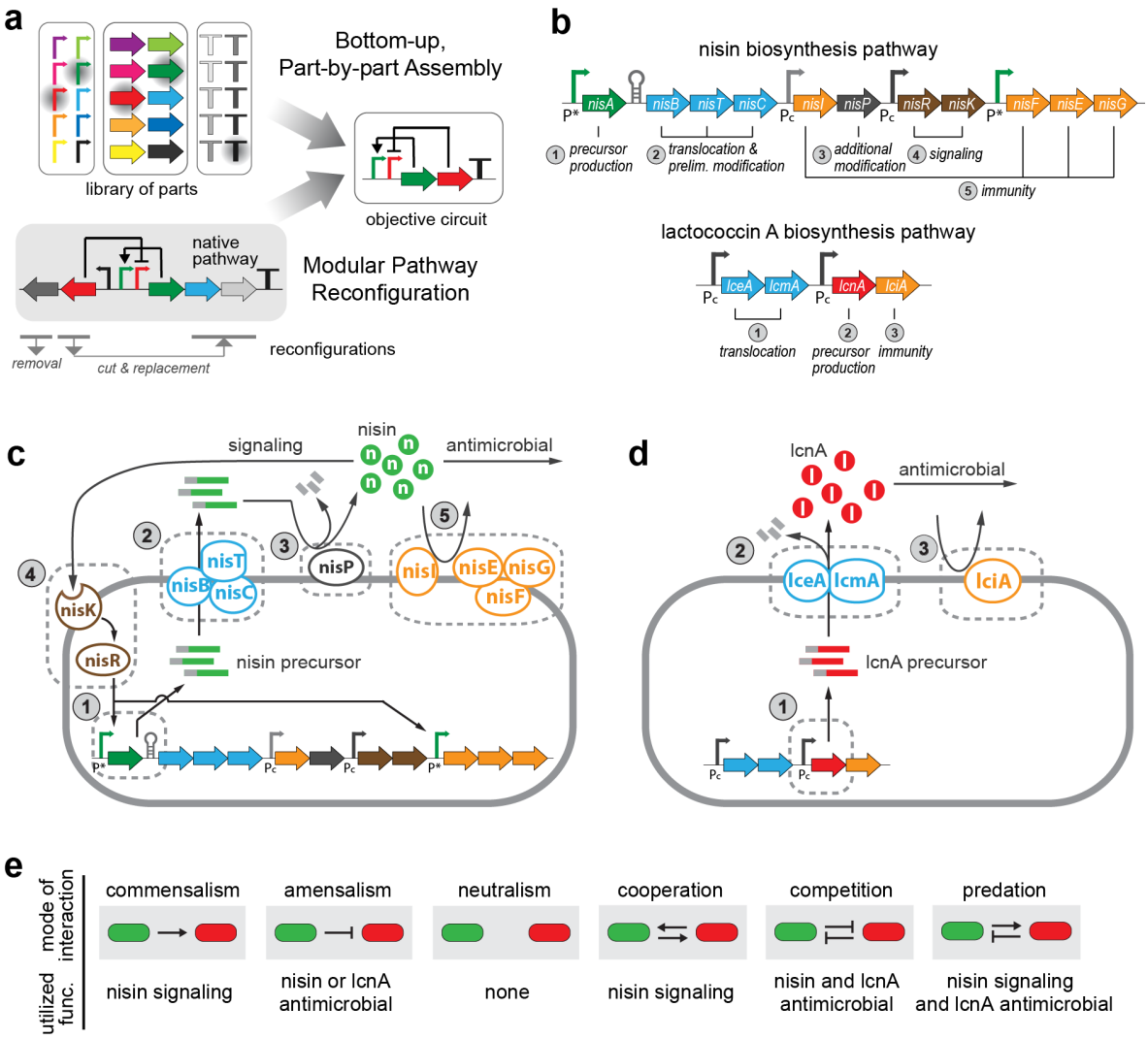

Figure 1: Modular pathway reconfiguration for engineering microbial consortia. (**a**) Two approaches to engineering gene circuits. A circuit can be created by assembling selected genetic parts from scratch or through modular reconfiguration of existing gene clusters. (**b**) nisin and lactococcin A (lcnA) biosynthesis gene clusters. (**c**) Modular organization of the nisin pathway. It involves five functionally independent modules, including those for precursor production (1), translocation and initial modification (2), additional modification (3), signaling (4), and nisin immunity (5). (**d**) Modular organization of the lcnA pathway. It contains three functionally independent

493 modules, including those for precursor production (1), translocation (2), and lcnA
494 immunity (3). (**e**) Design of six two-strain consortia that differentially utilize the signaling
495 and antimicrobial features of the bacteriocins.

Figure 2

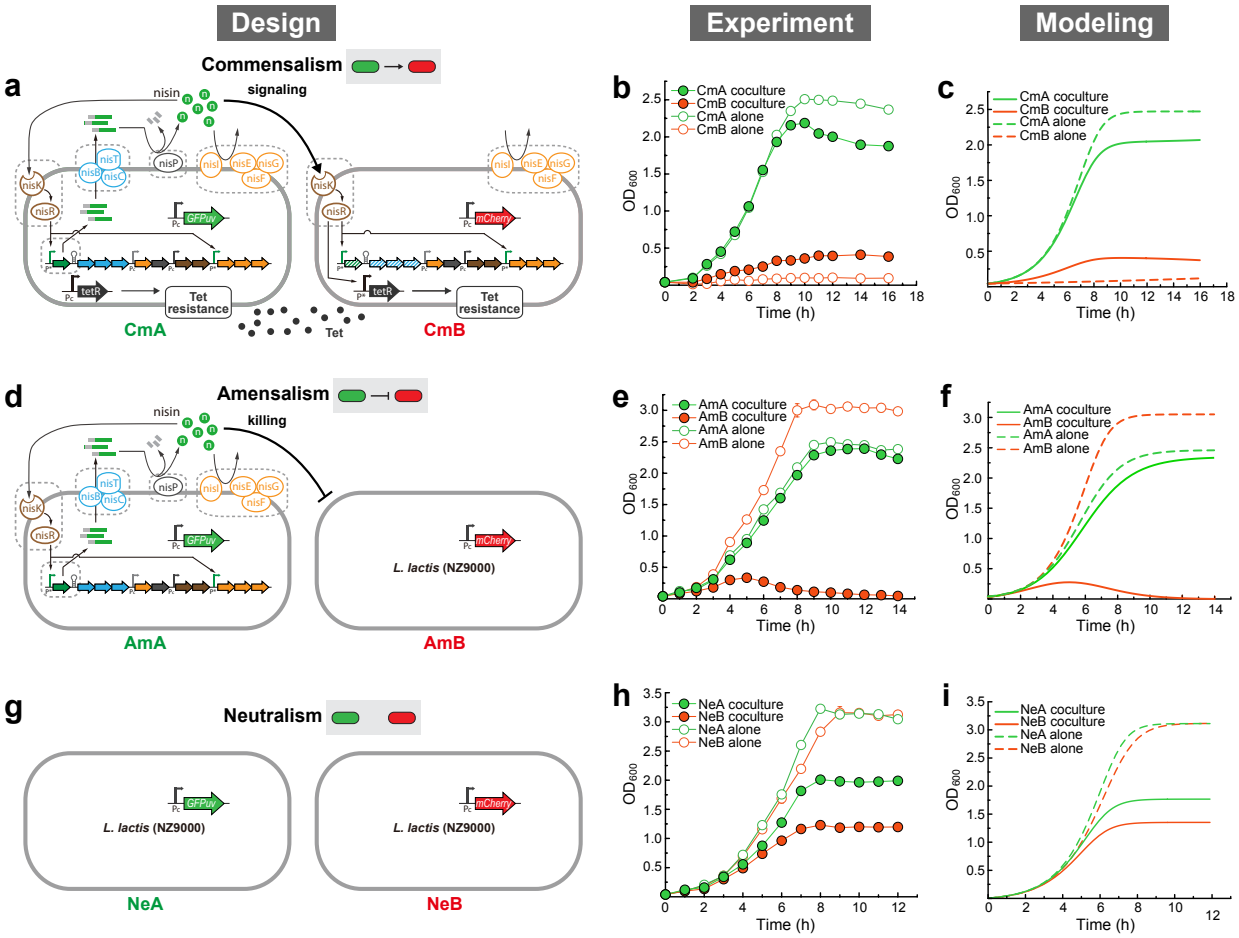

Figure 2: Synthetic consortia with one-way social interactions.

(**a**) Circuit diagram of a commensal microbial consortium. CmA is a nisin producer with constant tetracycline resistance. CmB has nisin-inducible tetracycline resistance. Here, genes filled with diagonal lines are knocked out. (**b**) Growth of CmA and CmB of the commensal consortium, in monoculture and co-culture experiments using GM17 media supplemented with tetracycline. (**c**) Simulated population dynamics for the commensal consortium. (**d**) Circuit diagram of a consortium of amensalism. AmA is a nisin producer that inhibits the growth of AmB. (**e**) Growth of AmA and AmB of the amensal consortium, in monoculture and co-culture experiments. (**f**) Simulated population dynamics for the consortium of amensalism. (**g**) Circuit diagram of a neutral consortium, where the two strains NeA and NeB do not have any active social interactions. (**h**) Growth of two neutral strains, NeA and NeB, in monoculture and co-culture experiments. (**i**) Simulated

population dynamics for the neutral consortium. In panels **b**, **e**, and **h**, closed and open circles stand for population growth in co- and monoculture experiments, respectively. In each co-culture experiment, strains were inoculated at 1:1 initial ratio. Experimental data are presented as mean (s.d.), n=3. In panels **c**, **f**, and **i**, dashed lines correspond to monoculture growth, while solid lines correspond to co-culture growth.

Figure 3

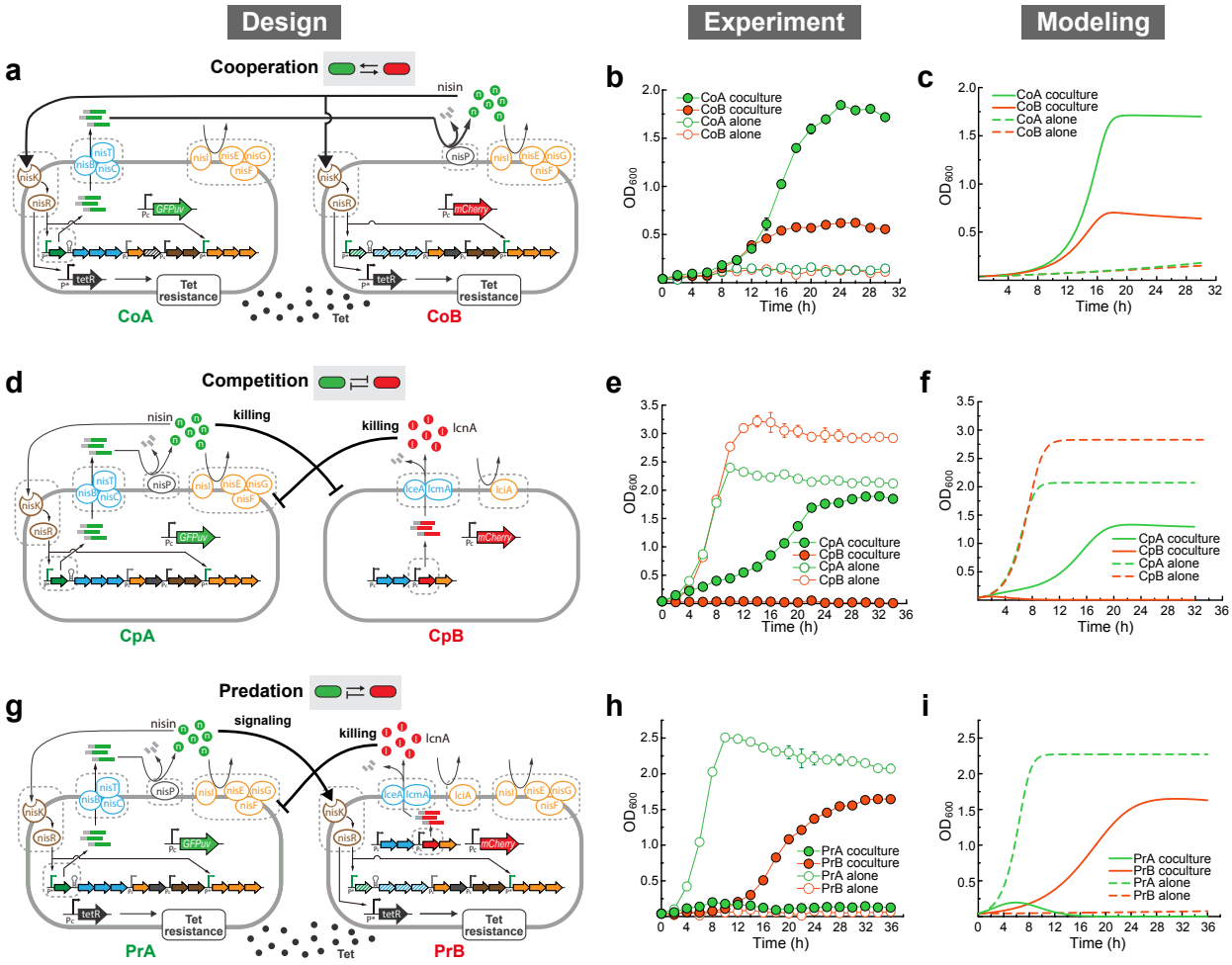

Figure 3: Synthetic consortia involving two-way social interactions.

(**a**) Circuit diagram of a cooperative consortium. CoA produces nisin precursor and CoB modifies the precursor to produce active nisin, forming a cooperation of successful nisin production. Nisin induces the tetracycline resistance of both strains, which enables them to survive in tetracycline-supplemented media. Here, genes filled with diagonal lines are knocked out. (**b**) Growth of two cooperative strains (CoA and CoB) in co-culture and monoculture experiments. (**c**) Simulated population dynamics for the cooperative consortium. (**d**) Circuit diagram of a mutually competitive consortium. CpA is a nisin producer and CpB is a IcnA producer. CpA outcompetes CpB in the co-culture experiment. (**e**) Growth of two competitive strains (CpA and CpB) in co-culture and monoculture experiments. (**f**) Simulated population dynamics for the competing

consortium. (**g**) Circuit diagram of a predative consortium. PrA (prey) is a nisin producer with constant tetracycline resistance. PrB (predator) is an lcnA producer with nisin-inducible tetracycline resistance. PrA induces the growth of PrB by secreting nisin; in turn, PrB suppresses the growth of PrA by releasing lcnA. Here, genes filled with diagonal lines are knocked out. (**h**) Growth of two predation strains, PrA and PrB, in co-culture and monoculture experiments. (**i**) Simulated population dynamics for the consortium of predation. In panels **b**, **e**, and **h**, closed and open circles stand for population growth in co-culture and monoculture experiments, respectively. In each co-culture experiment, strains were inoculated at 1:1 initial ratio. Experimental data are presented as mean (s.d.), n=3. In panels **c**, **f**, and **i**, dashed lines correspond to monoculture growth, while solid lines correspond to co-culture growth.

Figure 4

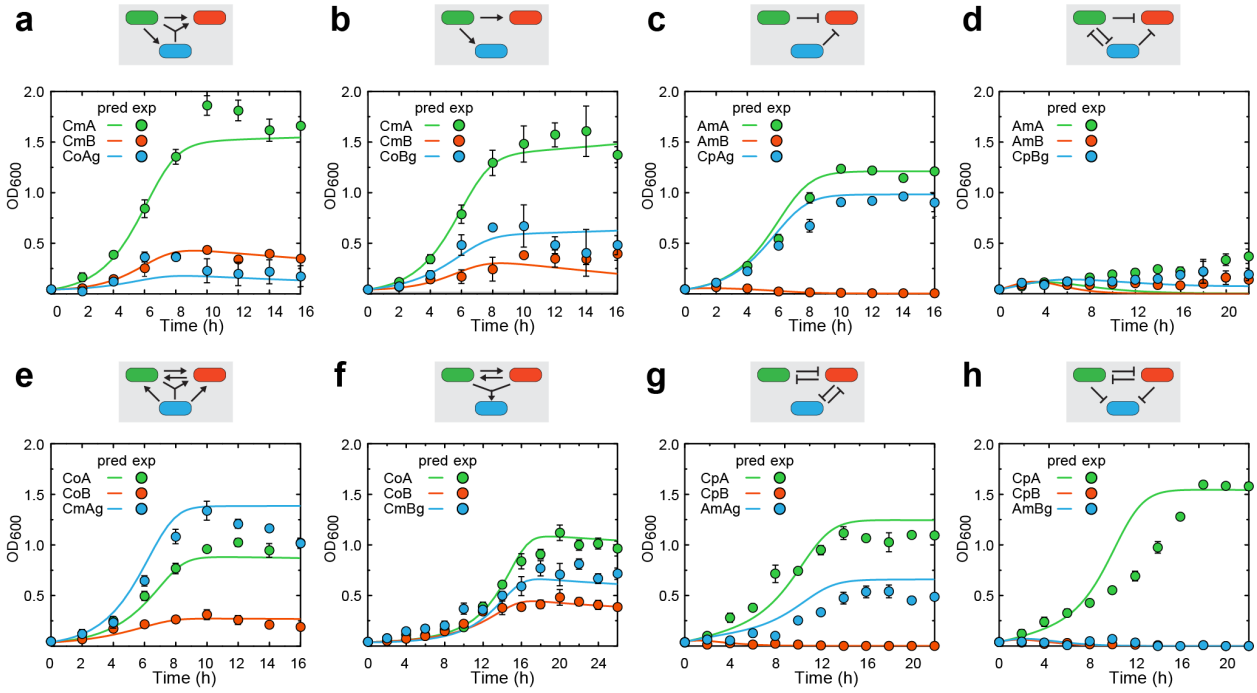

Figure 4: Model-predicted and experimentally measured population dynamics of three-strain ecosystems.

(**a**) Population dynamics of a three-strain consortium composed of the two commensalism strains (CmA and CmB) and a cooperation strain (CoAg). (**b**) Population dynamics of a three-strain consortium composed of the two commensalism strains (CmA and CmB) and a cooperation strain (CoBg). (**c**) Population dynamics of a three-strain consortium composed of the two amensalism strains (AmA and AmB) and a competition strain (CpAg). (**d**) Population dynamics of a three-strain consortium composed of the two amensalism strains (AmA and AmB) and a competition strain (CpBg). (**e**) Population dynamics of a three-strain consortium composed of the two cooperation strains (CoA and CoB) and a commensalism strain (CmAg). (**f**) Population dynamics of a three-strain consortium composed of the two cooperation strains (CoA and CoB) and a commensalism strain (CmBg). (**g**) Population dynamics of a three-strain consortium composed of the two competition strains (CpA and CpB) and an amensalism strain (AmAg). (**h**) Population dynamics of a three-strain consortium composed of the two competition strains (CpA and CpB) and an amensalism strain (AmBg). Each ecosystem's interaction network is shown on the top of the corresponding

559 panel. For all panels, lines and color circles stand for model predictions and
560 experimental results, respectively. Data are presented as mean (s.d.), n=3. In all co-
561 culture experiments, strains were inoculated at 1:1:1 initial ratio.
562

Figure 5

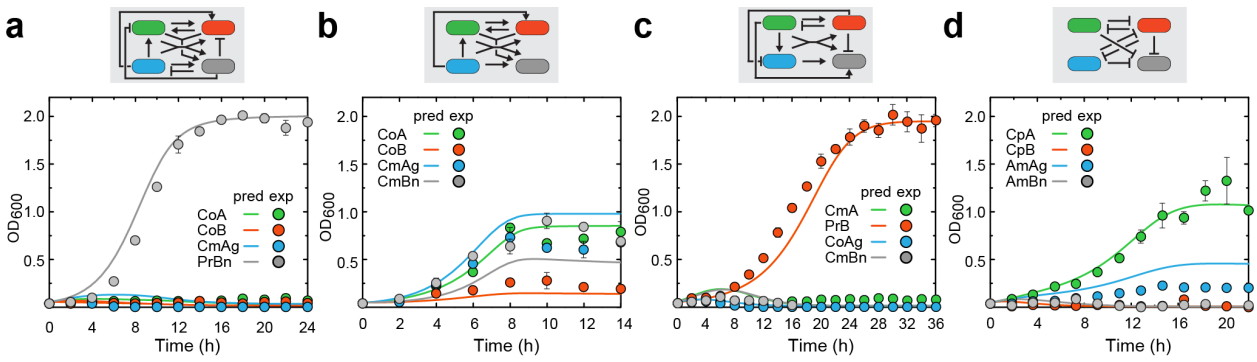

Figure 5: Model-predicted and experimentally measured population dynamics of four-strain ecosystems.

(**a**) Population dynamics of a four-strain consortium composed of two cooperation strains (CoA and CoB), a commensalism strain (CmAg) and a predation strain (PrBn). (**b**) Population dynamics of a four-strain consortium composed of two cooperation strains (CoA and CoB) and two commensalism strains (CmAg and CmBn). (**c**) Population dynamics of a four-strain consortium composed of two commensalism strains (CmA and CmBn), a predation strain (PrB) and a cooperation strain (CoAg). (**d**) Population dynamics of a four-strain consortium composed of two competition strains (CpA and CpB) and two amensalism strains (AmAg and AmBn). Each ecosystem's interaction network is shown on the top of the corresponding panel. For all panels, lines and color circles stand for model predictions and experimental results, respectively. Data are presented as mean (s.d.), n=3. In all co-culture experiments, strains were inoculated at 1:1:1:1 initial ratio.

Figure 6

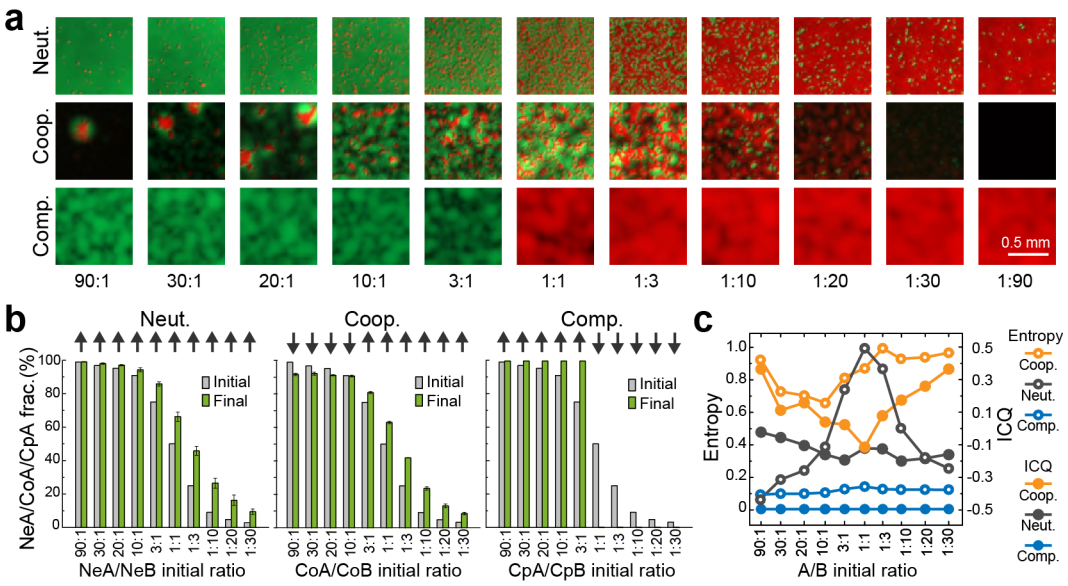

Figure 6: Spatial dynamics of three symmetrical communities.

(**a**) Spatial patterns emerged from the well-mixed consortia of neutralism, cooperation and competition growing on agar plates. A density of OD_{600}=0.2 and varied ratios from 90:1 to 1:90 were used as initial conditions. Each experiment was repeated at least three times. Representative pictures from the experiments are shown. (**b**) Comparison of the total initial and final population ratios of the consortia the experimental patterning processes. The NeA fraction increases in all cases due to a fast growth rate of NeA, the CoA fraction converged to ~90%, and CpA fraction diverged to either 100% or 0% depending on the initial conditions. Experimental data are presented as mean (s.d.), n=3. (**c**) Entropy (open circles) and intensity correlation quotient (ICQ) (closed circles) of the experimental patterns in panel **a**. The values of entropy and ICQ both follow the order of cooperation > neutralism > competition, although they are subject to initial conditions. Data are averaged from n=3 experiments. Each experiment was repeated at least three times. Representative pictures from experiments are shown.

Online Methods

Strains. *Lactococcus lactis* NZ9000 was used as host for strains in all ecosystems. Lactococcal strains were cultured in M17 medium with 0.5% glucose (GM17) at 30°C. All plasmids were first constructed and sequenced in *E. coli* NEB-10β, then transformed into *L. lactis* by electroporation. Antibiotics were added as required: chloramphenicol (10 μg ml^{-1}), erythromycin (250 μg ml^{-1}), tetracycline (3 μg ml^{-1}), kanamycin (50 μg ml^{-1}), spectinomycin (50 μg ml^{-1}), and streptomycin (150 μg ml^{-1}) for *E. coli*, and chloramphenicol (5 μg ml^{-1}), erythromycin (5 μg ml^{-1}), and tetracycline (10 μg ml^{-1}) for *L. lactis*. Please see Supplementary Table 1 for full strain and plasmid information.

Construction of the reporter and selector plasmids. Oligos for plasmid construction are listed in Supplementary Table 2. All reporter and selector plasmids were developed from an *L. lactis-E. coli* shuttle vector, pleiss-Nuc, which contains a pSH71 origin, a chloramphenicol resistance gene, a PnisA promoter from a nisin gene cluster, and a Nuc reporter[38]. Gibson assembly was used to construct all the reporter and selector plasmids. The plasmid for constitutively expressing GFP (pleiss-Pcon-gfp) was constructed by replacing PnisA promoter and Nuc in pleiss-Nuc with a *gfpuv* gene and the constitutive promoter of *lcnA*[30]. The plasmid for constitutive expression of RFP, pleiss-Pcon-rfp, was constructed by replacing *gfp* in pleiss-Pcon-gfp with *mcherry*. The selector plasmids pleiss-Pnis-tet-Pcon-gfp and pleiss-Pnis-tet-Pcon-rfp were constructed by amplifying tet^R gene from the plasmid pVPL3112 and Pcon-gfp or Pcon-rfp cassette from the plasmid constructed above and cloning them into pleiss-Nuc[39]. The tet^R gene was under the control of PnisA promoter. The plasmid pleiss-Pcon-tet-Pcon-gfp was constructed by insertion of tet^R and its RBS downstream of *gfp* in pleiss-Pcon-gfp. Both *gfp* and tet^R were under the control of the constitutive promoter of *lcnA*. The reporter and selector plasmids encoding a β–

glucuronidase (GusA)[40] were constructed by replacing *gfp* in the plasmids pleiss-Pnis-tet-Pcon-gfp and pleiss-Pcon-tet-Pcon-gfp with *gusA*. The reporter-free selector plasmids were constructed by deleting the *gfp* gene from pleiss-Pnis-tet-Pcon-gfp and pleiss-Pcon-tet-Pcon-gfp.

Construction of the plasmids for nisin production and nisin resistance. All nisin-producing plasmids in ecosystems were constructed based on the plasmid, pWK6, which was cloned by insertion of a wild-type nisin gene cluster from *L. lactis* k29 into pCCAMβ1; an *L. lactis-E. coli* shuttle vector[34,35]. To avoid leaky expression of promoter PnisA in cells provided with multi-copy *nisRK*, the *nisRK* gene in the multi-copy plasmid pWK6 was knocked out. In brief, the plasmids pWK6 and the Red/ET recombination plasmid pRedET (GeneBridges) were transferred into NEB-10β to generate the strain NEB-10β/pWK6/pRedET. Then the *aadA* gene (spectinomycin resistant gene) was amplified from plasmid pBeta[34] and the generating fragment was flanked with a short sequence of 3' of *nisP* and 5' of *nisF* and transformed into the induced competent cells of NEB-10β/pWK6/pRedET using the protocol described previously[34]. After recombination, the *nisRK* gene in pWK6 was replaced with the *aadA* gene, generating a new plasmid pWK6-RK$^-$. Then, pWK6-RK$^-$ was transferred into *L. lactis* NZ9000 (a single copy *nisRK* in its chromosome) to test the complementation and recovery of the nisin positive phenotype.

The plasmid pWK6 was also engineered to reduce its nisin productivity through reducing the RBS strength of *nisB* using ssDNA recombination performed as described previously[34]. In brief, a 90-nt ssDNA oligo nisB269 embracing an RBS sequence with a translation initiation rate (TIR) of 269 AU was designed using RBS calculator (https://salislab.net/software/). The ssDNA was transferred to the Beta protein expressing NEB-10β::MutS/pBeta/pWK6 to replace the wild-type *nisB* RBS (TIR=104148 AU) through

ssDNA recombination, thus generating the plasmid pWK6b. The plasmid pWK6b was further engineered to generate a *nisRK* knock-out version pWK6b-RK$^-$ according the method described above. Then, pWK6b-RK$^-$ was also transferred to *L. lactis* NZ9000 to test *nisRK* complementation.

The nisin resistant plasmid was developed based on pWK6. First, the start codon and RBS of *nisA* were mutated in pWK6 by ssDNA recombination using a 90-nt oligo nisAmut. Second, *nisP* and *nisRK* were knocked out by selection and counter-selection using a knstrep cassette as described previously[34]. Briefly, knstrep cassette flanking with 5' of *nisP* and 3' of *nisRK* was PCR amplified and transferred to NEB-10β/pWK6/pRedET replacing *nisPRK*. A fragment generated by fusion of a short fragment of 5' of *nisP* and 3' of *nisRK* using overlap extension PCR (OE-PCR) was transformed into the strain to replace knstrep by counter selection. Third, nisBTC was knocked out using the same method. The resulting plasmid was named pWK6-IFEG. Though pWK6-IFEG was unable to produce and modify nisin, it has all promoters and nisin immunity genes; it was transferred to *L. lactis* NZ9000 to test nisin immunity.

Construction of the plasmids for nisP$^-$ nisin precursor producer and nisP$^+$ nisin resistant strain. The NisP deficient prenisin synthesis plasmid for cooperation was constructed from the plasmid pWK6b. First, *nisP* and *nisRK* genes in pWK6b were knocked out by replacing them with knstrep cassette. Second, a fragment combining 5' of *nisP* and 3' of *nisRK* was generated by overlap extension PCR and used to replace the knstrep cassette by counter selection. The resulting plasmid was named pWK6b-PRK$^-$. The NisP+ nisin resistant plasmid for cooperation was generated from pWK6. First, start codon and RBS of *nisA* were mutated in pWK6 by ssDNA recombination using the 90-nt oligo nisAmut. Second, *nisRK* were knocked out by selection and counter selection using the knstrep

cassette. Third, *nisBTC* was knocked out by selection and counter selection. The resulting plasmid was named pWK6-IPFEG. Then, it was transferred to *L. lactis* NZ9000 to test nisin immunity. In addition, NZ9000/ pWK6b-PRK$^-$ and NZ9000/ pWK6-IPFEG were co-cultured at 1:1 ratio to examine their ability in cooperative production of nisin.

Construction of the plasmid for lcnA producer. Genes of lcnA gene cluster were amplified from plasmid pFI2396 and pFI2148 and assembled with P32 promoter into pleiss-Nuc vector in the following order: pleiss-3'-lciA-lcmA-lceA-Promoter-5'-5'-P32-lcnA-3'-pleiss (P32-lcnA has a different direction with other genes in the cluster)[41]. The RBS TIR of the precursor gene *lcnA* was changed by designing of RBS sequence with different TIR using RBS calculator. Then the lcnA gene cluster was amplified and subcloned to *Not* I site of pCCAMβ1 by Gibson assembly. Two variants pWK-lcnA^{5k} and pWK-lcnA^{20k} with TIR of 5078 AU and 19950 AU were chosen for subsequent experiments. In addition, genes of lcnA gene cluster were also assembled to wild-type gene cluster with their native promoters in original order in pleiss-Nuc vector. The wild-type gene cluster was then transferred to pCCAMβ1 to generate the plasmid pWK-lcnA^{wt}.

Construction of the plasmid with nisin resistance and lcnA gene cluster. The plasmid with both nisin resistance and lcnA production in predation was constructed by combining pWK-lcnA^{wt} and pWK6. First, pWK6 was engineered to *nisA* mutation, *nisBTC* knockout and *nisPRK* knockout by ssDNA recombination and selection and counter selection as mentioned above. Then, the modified nisin gene cluster with only nisin resistance function was amplified and cloned to *Not* I site of pWK-lcnA^{wt} through Gibson assembly. The resulting plasmid was named pWK6-IFEG-lcnA^{wt}.

Agar diffusion assay. All the nisin producer plasmids were transformed into *L. lactis* NZ9000. Agar diffusion assays were performed to measure nisin productivity of modified nisin producers and cooperative strains in cooperation as well as lcnA productivity of lcnA producers. Agar diffusion assay was performed as previously described[34] except a new *L. lactis* 117 indicator strain was used. The plasmid pCCAMβ1 (Erm^R) and pleiss-Pcon-tet-Pcon-gfp (Cm^R Tet^R) were co-transformed to *L. lactis* 117 so that it was resistant to erythromycin, chloramphenicol and tetracycline simultaneously. Then, the inhibition zone could affect the concentration of nisin in the culture without interference of antibiotics.

Co-culture experiments. Bacterial strains were grown overnight in GM17 media containing chloramphenicol and erythromycin to an early stationary phase. Bacteria were centrifuged and washed twice with fresh GM17 media. Then OD_{600} of the cells was adjusted to 2.0. Each strain in co-culture or monoculture was inoculated to fresh media with appropriate antibiotics at a 1:50 dilution. For neutralism, amensalism and competition, erythromycin and chloramphenicol were added. For commensalism, cooperation and predation, erythromycin and tetracycline were added for selection. Samples were taken from the cultures every two hours for measurement of growth. Meanwhile, cells from 500 µl of cultures were centrifuged and resuspended in PBS buffer. The cells were diluted to 10^6 cells ml^{-1} and stored in PBS buffer at 4°C for at least 4 hours then vigorously vortexed breaking most chains of lactococci into single cells. Then green and red fluorescent cells in the sample were counted by a Flow cytometer (BD LSR Fortessa). GFP was measured on the FITC channel, excited with a 488-nm blue laser and detected with a 530/30-nm bandpass filter. RFP was measured on PE-Texas Red channel using a 561-nm yellow/green laser and a 610/20-nm bandpass filter. At least 10,000 events were recorded for green and red cell counting per sample. In addition, images with green and red fluorescence were also taken by a

fluorescence microscope and at least 1000 cells from each sample were counted manually. The GusA-containing strains in the three- and four-strain consortia were distinguished by their blue color on GM17 agar plates containing 50 μg ml^{-1} of X-gluc (5-Bromo-4-chloro-3-indolyl beta-D-glucuronide sodium salt), and their colony forming units (CFUs) were counted to calculate their ratio in the population. For the no-color strains in four-strain consortia, their populations were obtained by subtracting the numbers of green, red and blue cells from the total populations. The growth curve of each strain in the population was drawn by multiplying total OD_{600} of the population with individual ratios. Control experiments with a single strain in commensalism, cooperation and predation induced with nisin was performed as follows: overnight cultures (diluted to OD_{600}=2.0) were inoculated to fresh GM17 media with erythromycin, tetracycline and 25 ng ml^{-1} of nisin (1 IU=25 ng) at a ratio of 1:50. Then the culture was incubated at 30°C and cell densities were measured at one or two hours' intervals.

Spatial patterns of well-mixed consortium droplets. Overnight single-strain cultures for neutralism, cooperation and competition were centrifuged and washed with fresh GM17 media. The cells were diluted to an OD_{600} of 0.2 using fresh media. Strain A and strain B in each ecosystem were mixed at different ratios from 90:1 to 1:90. Then 1 μl of the mixture was added onto a 90-mm agar plate (20 ml of GM17 agar with appropriate antibiotics and 2% agar). The plates were incubated at 30°C for different time. The incubation time was determined by the growth rate of strains in neutralism, cooperation (induced with 25 ng/ ml of nisin) and competition. The ratio of average growth rate of two strains in each consortium is 0.6 (Cooperation): 0.79 (Competition): 1 (Neutralism) in liquid culture. Cooperation with the lowest growth rate formed clear laws on agar after 45 h growth. Then the end point of experiment of the other two ecosystems was calculated based on this time: 35 h (~0.76 of

cooperation) for competition and 25 h (~0.6 of cooperation) for neutralism. Acquisition of images was performed with a Zeiss Axio V16 microscope using a HRm camera (Zoom 7×). The colonies grown from the droplets were subsequently picked up with an inoculating loop and dissolved in the PBS buffer. Ratios of strain A and strain B were counted by both plate pouring and flow cytometry. The spatiotemporal patterns of the predation ecosystem were obtained by spotting the well-mixed consortium droplets on the agar and taking images every 12 h with a Zeiss Axio V16 microscope.

Spatial patterns of structured consortium droplets. Overnight cultures were centrifuged and washed once with fresh media. The concentration of cells was diluted to an OD_{600} of 0.5 using fresh media. Then 0.5 μl of strain A and strain B in an ecosystem (neutralism, cooperation and competition) was added to a 90-mm agar plate (20 ml of 2% GM17 agar with appropriate antibiotics) with different distances. The plates were incubated at 30°C for different hours (25 h for neutralism, 45 h for cooperation and 35 h for competition). Acquisition of images was performed with a Zeiss Axio V16 microscope using a HRm camera (Zoom 7X).

Culture simulations. A general framework was constructed to describe the population dynamics of any two-strain community where the strains consume a common nutrient and interact through signaling molecules. Well-mixed culture models for six different social interactions (commensalism, amensalism, neutralism, cooperation, competition and predation) were first constructed modularly from the framework. These models were fit to experimental data, then recombined modularly to predict three- and four-strain ecosystems. Whenever possible equations and parameters were reused to reflect the modular construction of the ecosystems. MATLAB was used to produce plots, analyze images and fit

776 data for the models. Data from supplemental control experiments were also used to fit
777 parameters.
778
779 **Spatial simulations.** A general framework was constructed to describe the spatiotemporal
780 dynamics of any two-strain community which involves nutrient co-utilization and active
781 social interactions through diffusible signaling molecules. All three symmetric ecosystems
782 (neutralism, cooperation and competition) were constructed modularly to reflect the modular
783 reconfiguration concept of the ecosystem engineering. Each ecosystem was simulated
784 using C++ and analyzed in MATLAB. The entropy and co-localization of bacterial strains
785 were also measured and plotted.
786
787 **Statistical analysis.** All of the experiments were performed for at least three times.
788 Replicate numbers of the experiments (n) are indicated in the figure legends. Sample sizes
789 were chosen based on standard experimental requirement in molecular biology. Data are
790 presented as mean ± s.d. Fluorescence microscopy images are representatives of the
791 images from multiple experimental replicates.
792
793 **Life Sciences Reporting Summary.** Further information on experimental design is
794 available in the Life Sciences Reporting Summary.
795
796 **Code and Data availability.** Custom C++ and MATLAB codes developed in this study and
797 data supporting the findings of this study are available within the paper and its
798 supplementary information files or from the corresponding author upon reasonable request.
799 Sequences of plasmids are available at GenBank under the following accession numbers:
800 pWK6, MG913135; pWK6-RK^{-}, MG913136; pWK6b-PRK^{-}, MG913137; pWK-lcnA^{wt},

MG913138; pWK-lcnA^{5k}, MG913139; pWK-lcnA^{20k}, MG913140; pWK6-IFEG, MG913141; pWK6-IPFEG, MG913142; pWK6-IFEG-lcnA^{wt}, MG913143.

References

38. Le Loir, Y., Gruss, A., Ehrlich, S. & Langella, P. A Nine-Residue Synthetic Propeptide Enhances Secretion Efficiency of Heterologous Proteins in *Lactococcus lactis*. *J. Bacteriol.* **180**, 1895-1903 (1998).

39. Oh, J.-H. & van Pijkeren, J.-P. CRISPR–Cas9-assisted recombineering in *Lactobacillus reuteri*. *Nucleic Acids Res.* **42**, e131 (2014).

40. Douglas, G.L. & Klaenhammer, T.R. Directed Chromosomal Integration and Expression of the Reporter Gene *gusA3* in *Lactobacillus Acidophilus* NCFM. *Appl. Environ. Micobiol*. **77**, 7365-7371 (2011).

41. Fernández, A., Horn, N., Gasson, M.J., Dodd, H.M. & Rodríguez, J.M. High-level coproduction of the bacteriocins nisin A and lactococcin A by *Lactococcus lactis*. *J. Dairy Res.* **71**, 216-221 (2004).